

## A Vortex-Based Perspective of Eastern Pacific Tropical Cyclone Formation

CHRISTOPHER DAVIS AND CHRIS SNYDER

*National Center for Atmospheric Research, Boulder, Colorado*

ANTHONY C. DIDLAKE JR.

*University of Washington, Seattle, Washington*

(Manuscript received 24 July 2007, in final form 24 October 2007)

### ABSTRACT

Tropical cyclone formation over the eastern Pacific during 2005 and 2006 was examined using primarily global operational analyses from the National Centers for Environmental Prediction. This paper represents a “vortex view” of genesis, adding to previous work on tropical cyclone formation associated with tropical waves. Between 1 July and 30 September during 2005 and 2006, vortices at 900 hPa were tracked and vortex-following diagnostic quantities were computed. Vortices were more abundant during periods of an enhanced “Hadley” circulation with monsoon westerlies around 10°N in the lower troposphere. This zonally confined Hadley circulation was significantly stronger during the genesis of developing vortices. Developing vortices were stronger at the outset, with a deeper potential vorticity maximum, compared to nondeveloping vortices. This implies that developing disturbances were selected early on by favorable synoptic-scale features.

The characteristic time-mean reversal of the meridional gradient of absolute vorticity in the lower troposphere was found to nearly vanish when the aggregate contribution of strong vortices was removed from the time-mean vorticity. This finding implies that it is difficult to unambiguously attribute development to a preexisting enhancement of vorticity on the synoptic scale. The time-mean enhancement of cyclonic vorticity primarily results from the accumulated effect of vortices. It is suggested that horizontal deformation in the background state helps distinguish developing vortices from nondevelopers, and also biases the latitude of development poleward of the climatological ITCZ axis.

### 1. Introduction

In no region on earth is the occurrence of tropical cyclone formation more confined geographically than over the eastern North Pacific Ocean. Nearly  $\frac{3}{4}$  of the eastern Pacific storms form within a small longitudinal range, 95–115°W, and a narrow latitudinal extent, 8–16°N. Maloney and Hartmann (2000, 2001) indicated that genesis is favored when the Madden–Julian oscillation (MJO) is in its westerly phase over the eastern Pacific. Molinari and Vollaro (2000) added that the combination of easterly waves traversing Central America into the eastern Pacific and westerlies near 10°N produced a significant enhancement of environmental vorticity whereby development was more likely

and more rapid. Enhanced convection in this lower-tropospheric westerly regime was attributed to enhanced surface fluxes within strengthened cross-equatorial flow (Raymond et al. 2006). Enhanced convection prior to genesis, represented by decreased outgoing longwave radiation (OLR), has been found to be a coincident property of the MJO, equatorial Rossby waves, and mixed Rossby–gravity modes (including easterly waves) prior to genesis over the eastern Pacific (Frank and Roundy 2006).

To date, there have been no published studies that distinguish between developing and nondeveloping waves or vortices over the eastern Pacific. One of the most complete comparisons of developing and nondeveloping tropical disturbances, McBride and Zehr (1981), says nothing about this region. In the Atlantic and western Pacific basins, McBride and Zehr showed that disturbances in their sample were identified with lower-tropospheric cyclonic circulations or vortices. It is reasonable to define nascent disturbances over the

---

*Corresponding author address:* Christopher A. Davis, National Center for Atmospheric Research, P.O. Box 3000, Boulder, CO 80307.

E-mail: cdavis@ucar.edu

eastern Pacific as vortices as well, in addition to any wavelike characteristics they may have on the synoptic scale. The primary motivation for the present paper is to examine synoptic-scale conditions associated with both developing and nondeveloping vortical disturbances over the eastern Pacific, and elucidate factors that distinguish one from the other.

The documented factors favoring the development of tropical cyclones (e.g., Gray 1968; DeMaria et al. 2001) include a high sea surface temperature, moist midtroposphere, strong divergence in the upper troposphere, weak vertical wind shear, and preexisting cyclonic vorticity in the lower troposphere. There are two issues regarding such parameters. First, several of them are correlated, particularly divergence, vorticity, and midtropospheric moisture. They are related through vertical circulations, especially those driven by condensation heating. Such circulations can occur on synoptic scales (Rosenthal 1967), such as within the intertropical convergence zone (ITCZ), a monsoon trough, convectively coupled waves, and intraseasonal oscillations. Or, they can occur on the mesoscale within mesoscale convective systems. This “scale degeneracy” is the other issue, namely, that there is ambiguity between what is the environment and what is the disturbance. To some extent, relationships between variables transcend the synoptic scale to the mesoscale. Similarly “favorable” values of vorticity, divergence, and humidity characterize both the synoptic-scale region within which a tropical cyclone may form and the nascent cyclone itself. The issue of separating a disturbance, developing or not, from its synoptic-scale surroundings, will be considered directly in the present study. Furthermore, the interrelationships between variables on larger scales will be clarified from a phenomenological perspective.

The present study presents a “vortex based” perspective of tropical cyclone formation, an alternative to the wave-based perspective of genesis. The present paper makes no attempt to select either perspective as a preferred framework for genesis. Rather, both are acknowledged and complementary in the sense that waves can contain vortices (Berry and Thorncroft 2005). By focusing on vortices, it is intended that a portion of the conceptual bridge between the large-scale and mesoscale dynamics of hurricane genesis be constructed.

Global analyses, supplemented or evaluated with limited special observations, are used to composite developing and nondeveloping eastern Pacific vortices. An automated vortex identification and tracking algorithm is applied to identify objectively vortices and allow system-relative compositing of environmental characteristics in both developing and nondeveloping

samples. The time period July–September during both 2005 and 2006 is examined.

After describing, in section 2, the global analyses, a case study of the development of tropical storm Eugene (2005) is presented. In section 3, the context for this development is examined by comparing synoptic-scale conditions for developing and nondeveloping vortices detected and tracked during two hurricane seasons. The importance of an enhanced “Hadley” circulation in developing cases is emphasized, primarily through its effect on deep tropospheric humidity. Furthermore, it is suggested that reduced horizontal deformation in the environment, perhaps more than relative vorticity, favors development poleward of the ITCZ. Numerous vortices within the ITCZ are stretched zonally in deformation and typically do not develop.

## 2. Eugene

The data used in this study consist mostly of the National Centers for Environmental Prediction (NCEP) final operational analyses archived on a  $1^\circ \times 1^\circ$  grid at 6-hourly intervals. These data are available on 27 pressure levels. (Details about the analyses may be found online at <http://www.emc.ncep.noaa.gov/modelinfo/>.) Herein, these analyses will be referred to as the Global Data Assimilation System (GDAS) analyses. To facilitate diagnostic analysis, these data were interpolated to a Mercator projection grid with 90-km spacing.

To be a viable tool in this study, the GDAS analyses must represent vortices and the fields that accompany them realistically, particularly winds at lower-tropospheric and upper-tropospheric levels, and moisture anomalies in the midtroposphere. Observations such as satellite winds from multiple geostationary platforms are assimilated, with the Geostationary Operational Environmental Satellites (GOES) providing coverage over the eastern Pacific. An example of winds at 200 hPa derived from tracking cloud motions using infrared radiances appears in Fig. 1. This time, 0000 UTC 17 July 2005, is 30 h prior to the first location of tropical depression Eugene in the best-track data. The location of the vortex precursor to tropical storm Eugene at 1200 UTC 17 July is indicated. Apparent in both the analyzed and satellite-derived winds is strong northeasterly flow across an extensive longitudinal range to the south of where Eugene developed. There is clearly quantitative agreement between the analysis and satellite-derived winds.

In this particular case, dropsondes were deployed by the National Oceanic and Atmospheric Administration (NOAA) P-3 Orion aircraft during an investigation of a possible vortex during the National Aeronautics and

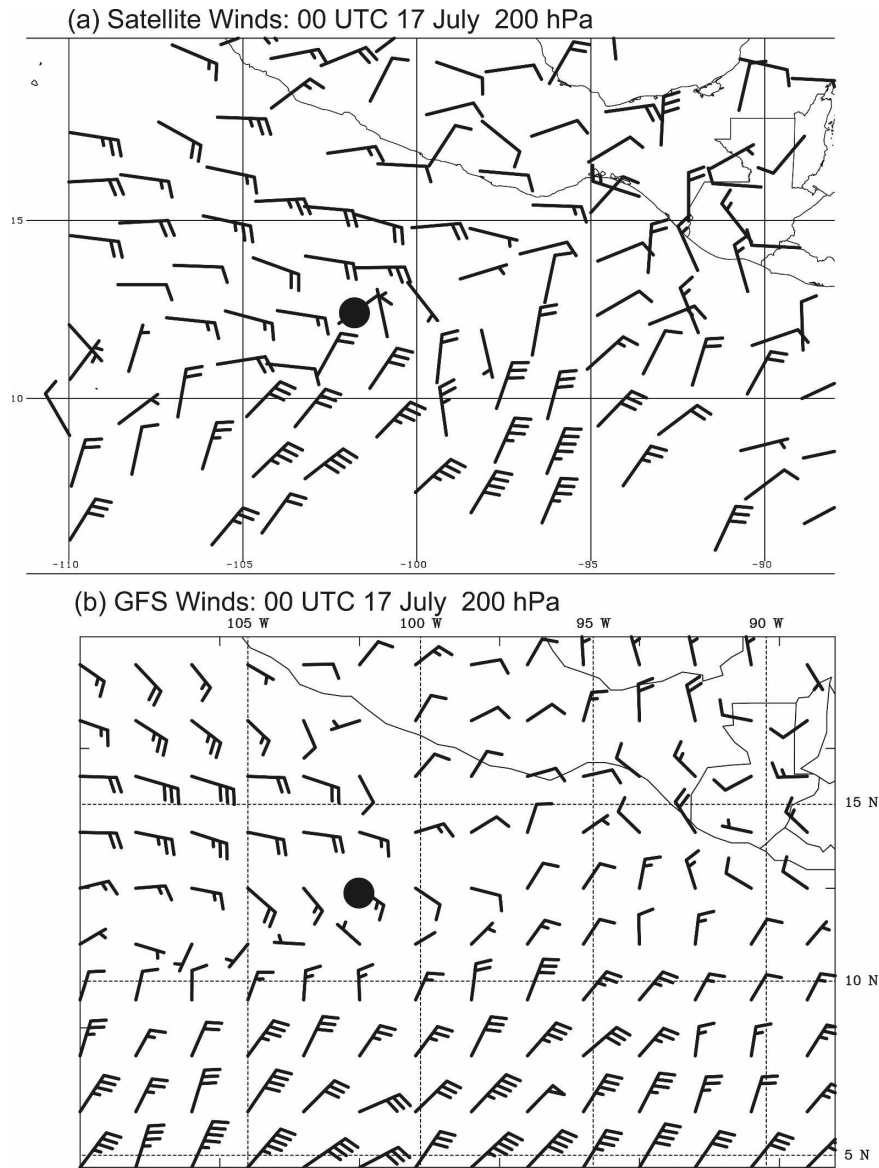


FIG. 1. (a) Infrared-radiance-derived satellite winds at 200 hPa valid at 0000 UTC 17 Jul 2005, obtained from the Space Science and Engineering Center at the University of Wisconsin; (b) 200-hPa winds from GDAS analysis, also valid at 0000 UTC 17 Jul 2005. The long barb equals 10 kt. The black dot locates the pre-Eugene vortex at 1200 UTC 17 Jul 2005.

Space Administration (NASA) Tropical Cloud Systems and Processes (TCSP) field study (Halverson et al. 2007). Data collected between 1700 and 2300 UTC 15 July were time-space corrected to 1800 UTC 15 July, assuming a westward motion of  $3 \text{ m s}^{-1}$  (see Fig. 4), and are compared to the 1800 UTC GDAS analysis in Fig. 2b. The dropsonde data are consistent with the GDAS analysis at 900 hPa indicating a vortex centered near  $10^\circ\text{N}$ ,  $87^\circ\text{W}$ , with another vortex farther northwest. The dropsondes data were available for assimilation in the GDAS analyses, so agreement might not be surprising.

However, the eastern vortex was already well defined in the analysis at 1200 UTC (Fig. 2a), having intensified in successive analyses during the previous night in association with nocturnal convection. The realistic development of a vortex in this case implies that the analysis is capable of representing such features.

Eugene was recognized by the National Hurricane Center (NHC) as a tropical depression at 0600 UTC 18 July and as a tropical storm 6 h later. However, as the sequence of satellite images in Fig. 3 indicates, a substantial increase in convection activity and a northward

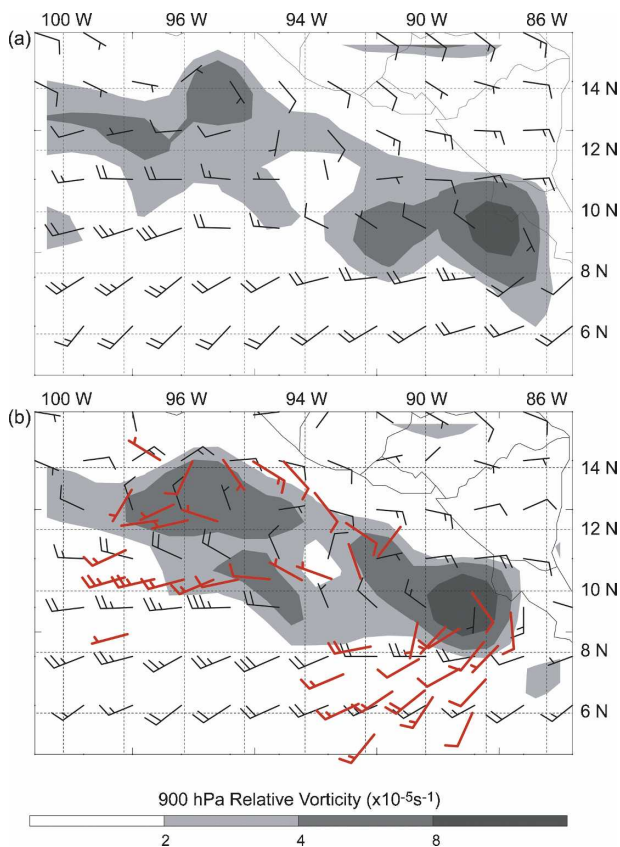


FIG. 2. GDAS analysis wind at 900 hPa valid at (a) 1200 and (b) 1800 UTC 15 Jul 2005. Dropsonde winds at 900 hPa, time-space corrected to 1800 UTC appear in red. Shading indicates GDAS relative vorticity at 900 hPa.

migration of the ITCZ became evident more than 2 days prior to the formation of Eugene. At 1800 UTC 14 July, the ITCZ could be identified as a nearly continuous band of cirrus along 12°N latitude. On 15 July, a northward bulge in the ITCZ became evident, along with a meridional expansion of deep cloud as far as 15°N. Once perturbed, this portion of the ITCZ remained poleward of its initial position until after Eugene developed on 18 July. Extending over 3000 km in the east–west direction, the band of enhanced convection moved westward with time at a speed of between 8 and 10  $\text{m s}^{-1}$ . Convection quickly dissipated to the east of Eugene following the cyclogenesis.

Vorticity plotted every 24 h beginning 1800 UTC 14 July (Fig. 4) reveals the northward bulge of the ITCZ about 2 days prior to genesis. In this process, convection was enhanced within a zonally elongated region poleward and eastward of the strongest southerlies. Vortices formed in the convection region (Figs. 4b,c), and qualitatively resembled solutions to the barotropic instability of a potential vorticity (PV) strip (Ferreira

and Schubert 1997). Note that such a PV strip did exist (Fig. 5). However, the time scale of vortex formation was of the order of 1 day or less, and the spacing of the vortices was only about 500 km. These temporal and spatial scales were roughly 4–5 times smaller than one expects from barotropic instability. Therefore, it is unlikely that barotropic instability is the best theoretical model to explain the proliferation of vortices along the ITCZ in this case.

Further examination of Fig. 4 reveals two characteristic speeds of westward movement. Individual vortices, such as the one found near the Costa Rican coast at 1200 UTC 15 July (Figs. 2b and 4b) and the vortex that became Eugene (Figs. 4a–e), moved westward at approximately 3  $\text{m s}^{-1}$ . There was also westward movement of a zonally elongated region of enhanced cyclonic vorticity at roughly 8–10  $\text{m s}^{-1}$ . This area coincided approximately with the region of enhanced convection in Fig. 3. East of 95°W, northerly winds became evident on 17 July and expanded westward at roughly the same speed of 8–10  $\text{m s}^{-1}$ . The existence of a westward-propagating wave, apparently equatorially trapped owing to its lack of definition poleward of approximately 10°N, is strongly suggested. However, it is difficult to uniquely identify the wave type, and it is likely that more than one type of tropical wave was involved (Frank and Roundy 2006). For instance, there is evidence in OLR data of an eastward-propagating convectively coupled Kelvin wave affecting the genesis region from 11 to 15 July (not shown). The potential influence of this feature on the evolution of the ITCZ and its relation to the apparent westward-moving wave is not considered herein, but more detailed investigation of these wave features could better link the vortex evolution prior to Eugene to the synoptic-scale wave dynamics.

### 3. Statistics from the 2005 and 2006 seasons

Having briefly examined one example of genesis over the eastern Pacific, it is important to place this event into a proper context by examining a significant sample of cases. Furthermore, since this paper is focused on distinguishing developing and nondeveloping tropical systems, objective criteria must be established by which both sets of disturbances may be identified. The relative vorticity at 900 hPa in the GDAS analysis is the variable used to define vortices. The period of interest is restricted to July–September during 2005 and 2006.

Relative vorticity was first smoothed by replacing the value at each grid point by the average over a  $5 \times 5$  stencil centered on that point ( $450 \times 450$  km). All maxima of smoothed vorticity exceeding  $1.5 \times 10^{-5} \text{ s}^{-1}$

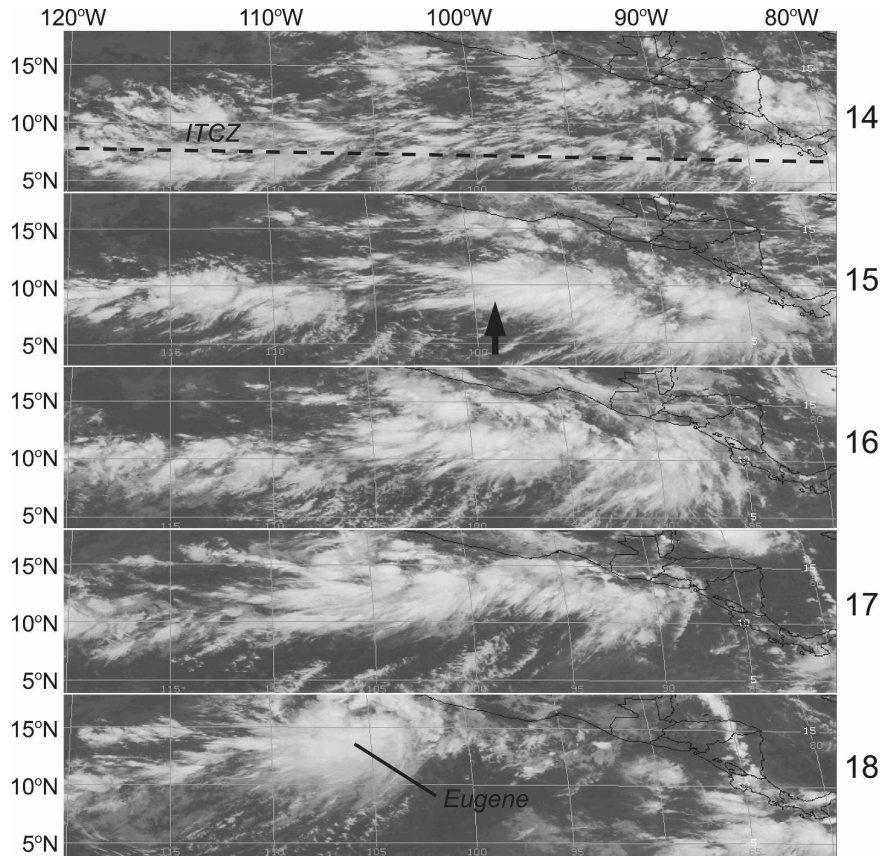


FIG. 3. Infrared satellite images from *GOES-11* at 1800 UTC 14–18 Jul 2005. (from top to bottom) The dashed line indicates the initial position of the ITCZ and the arrow points to the northward bulge in the ITCZ.

were then located.<sup>1</sup> The extent of the cyclonic vorticity region was determined in each of the Cardinal directions as the distance to where the vorticity fell to 0.2 times its maximum value or to where the vorticity stopped decreasing with distance from the central maximum.

Once identified, vortices were tracked. Consider all vortices identified at analysis time  $t_0$ . The position of each vortex was extrapolated linearly to the next analysis time  $t_0 + \delta t$  using its movement within the past 12 h ( $t_0 - 12$  h). At  $t + \delta t$ , all vortices were identified in the same manner as at  $t_0$ . If the position of any vortex at  $t_0 + \delta t$  fell within 270 km (three grid points) of the extrapolated position of any vortex from  $t_0$ , these were identified as the same vortex, and the track of vortex at  $t_0$  was extended to its position at  $t_0 + \delta t$ . If the extrapolated position of a vortex was not within 270 km of any

vortex at  $t_0 + \delta t$ , the track terminated at  $t_0$ . If a vortex analyzed at  $t_0 + \delta t$  was not within 270 km of any extrapolated position from  $t_0$ , a new vortex was identified at  $t_0 + \delta t$ .<sup>2</sup> Only vortices that existed over eastern Pacific waters were considered. Although some may have formed farther east, each track began when the vortex was first over the eastern Pacific. This filtered out land-falling Atlantic tropical systems, of which there were several in 2005.

Wang and Magnusdottir (2006) noted that the ITCZ was often characterized by local enhancements of cyclonic vorticity. They found that these enhancements more often appeared as coherent vortices in the GDAS analysis than in data from the Quick Scatterometer (QuikSCAT). However, there was a high degree of cor-

<sup>1</sup> This vorticity threshold was approximately one-tenth the largest value of smoothed vorticity in the dataset.

<sup>2</sup> Tracks of long-lived, vortices were also examined subjectively to identify possible breaks in tracks due to ambiguities in identifying vortices at a single analysis time. In two instances, both developing cases, a broken track was reconnected.

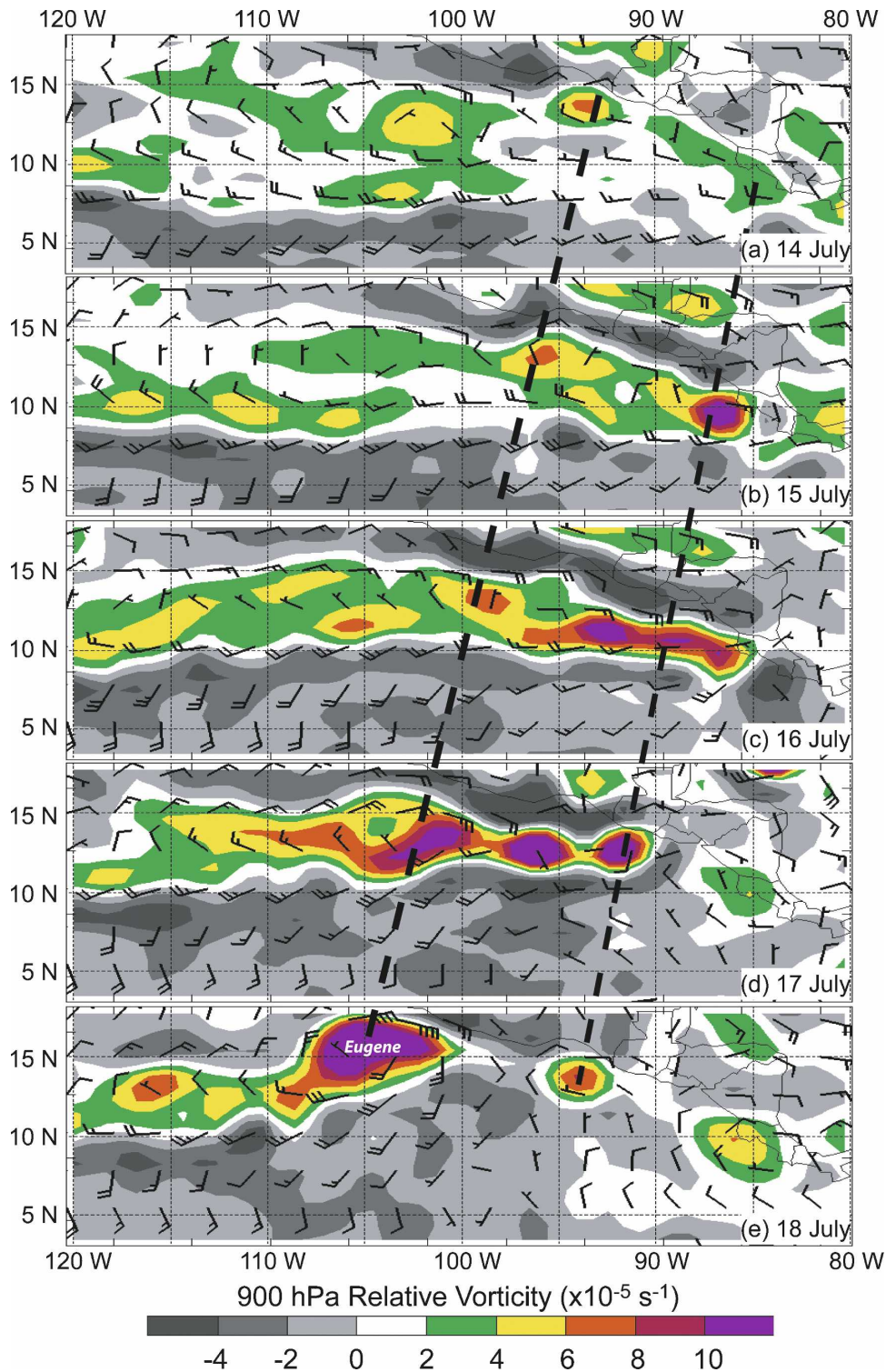


FIG. 4. Relative vorticity and wind at 900 hPa at 24-h intervals beginning at 1800 UTC 14 Jul 2005. Times correspond to those in Fig. 3. Heavy dashed lines indicate approximate motion of individual vortices (about  $3 \text{ m s}^{-1}$ ). The more western of the two developed into Eugene.

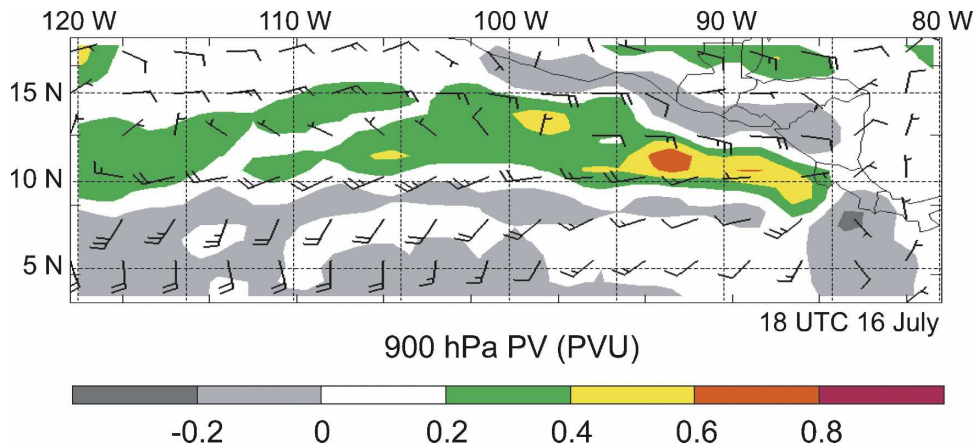


FIG. 5. Potential vorticity at 900 hPa (PVU, 1 PVU =  $10^{-6} \text{ m}^2 \text{ K kg}^{-1} \text{ s}^{-1}$ ) at 1800 UTC 16 Jul 2005.

response between vortices in the GDAS and enhanced vorticity patches along the ITCZ in QuikSCAT.

Restricting attention to vortices exceeding our detection threshold for 2 days, forming east of  $150^\circ\text{E}$  over the waters of the Pacific Ocean, a total of 60 disturbances were found between July and September 2005, and 52 were found during the same period in 2006. The number of developing storms was 12 during each 3-month period. In most instances of developing storms, the vortex track began prior to the start of official NHC track. In 2005, the median time between

first vortex identification and first best-track identification was 24 h. In 2006, that time increased to 42 h. Thus, the first 48 h after detection in the GDAS analyses is accurately described as the genesis phase.

Herein, statistical and spatial distributions of several quantities are presented, some in a vortex-following coordinate system, to highlight differences between developing and nondeveloping vortices. The distributions of vortex strength and vortex longevity, and their covariance, can be discerned from Fig. 6. Vortex strength is the smoothed vorticity used for detection, also aver-

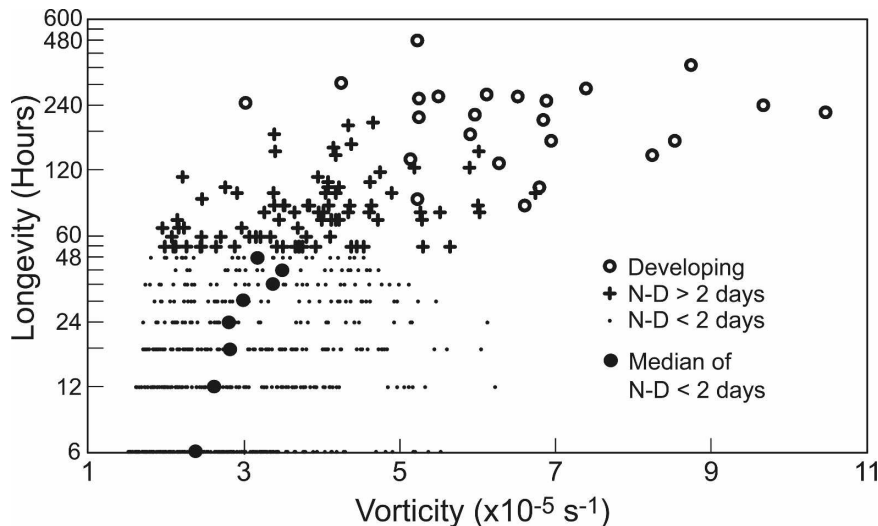


FIG. 6. Vorticity of each vortex during July–September 2005–06 exceeding  $1.5 \times 10^{-5} \text{ s}^{-1}$  (averaged over a  $450 \times 450 \text{ km}$  box) plotted against vortex longevity (logarithmic scale). Vorticity values are averaged over the first 48 h for vortices lasting 2 or more days, or averaged over the entire life cycle if lasting less than 2 days. Open circles denote developing vortices and the plus signs denote nondeveloping vortices lasting 2 or more days. Dots denote vortices lasting less than 2 days. Filled circles indicate the median vorticity among short-lived vortices with the same lifetime.

aged over the first 48 h following the first detection time for each vortex. Short-lived vortices are defined as existing less than 2 days (dots), and their vorticity value is an average over their lifetime. The vorticity values thus obtained are referred to as “initial vorticity.” It is seen that all vortices whose initial vorticity exceeds  $7 \times 10^{-5} \text{ s}^{-1}$  become tropical cyclones. Conversely, it is rare for vortices initially weaker than  $5 \times 10^{-5} \text{ s}^{-1}$  to develop. Note that an average vorticity of  $7 \times 10^{-5} \text{ s}^{-1}$  over a box 450 km on a side is equivalent to a cyclonic circulation averaging about  $8 \text{ m s}^{-1}$  around the perimeter of the box. The maximum winds are larger than this value. Studies such as Rotunno and Emanuel (1987) have demonstrated that initial disturbances of approximately this strength are unstable whereas disturbances with tangential winds of only a few meters per second are stable. The main point of Fig. 6 is that the longevity of vortices, and their outcome regarding genesis, are strongly influenced by their intensity (vorticity) soon after detection. This result is consistent with the finding of DeMaria et al. (2004), that lower-tropospheric vorticity in the GDAS analysis is a good predictor of tropical cyclone formation.

A composite vertical structure of PV valid 24 h after detection of each vortex was constructed (Fig. 7), and separated into two samples: the 24 developing vortices and the 24 weakest nondeveloping vortices lasting at least 2 days. The 24 weakest nondeveloping cases were selected to provide greater contrast with developing cases than would be seen from the entire sample of nondevelopers. The deeper, more intense, potential vorticity signatures belonged to the developing vortices. The PV tower in developing cases extended to almost 400 hPa. While shallower, broader, and weaker than the PV tower of a typical hurricane, the likeness of vertical structure implies that developing vortices were already on the path to becoming tropical cyclones soon after they were first observed. If genesis were a random process on the mesoscale, we might expect to see less distinction between developing and nondeveloping cases at the outset. On the contrary, developing vortices are “selected” early on, suggesting a fundamental role of the synoptic-scale environment.

The spatial relationship of developing and nondeveloping systems to the large-scale, zonal flow, as depicted in a time–latitude format (Fig. 8), is such that both developing and nondeveloping systems appear more frequently in periods of enhanced westerlies in the lower troposphere. However, nondeveloping vortices cluster between  $8^\circ$  and  $10^\circ\text{N}$ , whereas developing vortices are centered approximately  $4^\circ$  poleward of the nondeveloping vortices. In agreement with Maloney

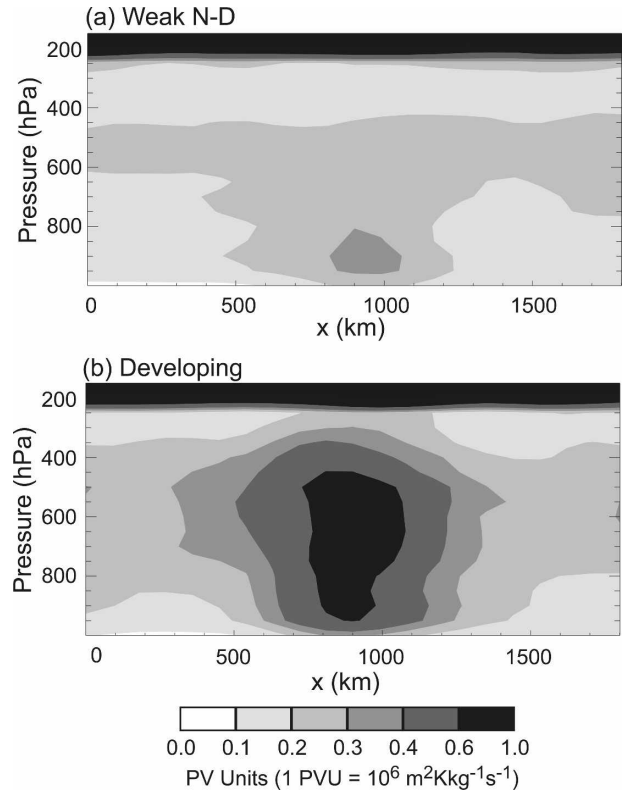


FIG. 7. GDAS analyzed composite potential vorticity (PVU) along east–west cross sections through the vortex: (a) 24 weakest nondeveloping vortices and (b) 24 developing vortices. Each composite is valid 24 h after the initial vortex detection.

and Hartmann (2000, 2001), development does not occur during periods of easterlies, however, some nondeveloping vortices occur during periods of easterlies.

The intraseasonal intermittency of the westerlies at  $10^\circ\text{N}$  is clearly an important factor governing tropical cyclone formation. The MJO has been shown to contribute to this intraseasonal variability (e.g., Maloney and Hartmann 2000, 2001; Molinari and Vollaro 2000), but there is not always a clear signal of MJO propagation east of the date line (e.g., Zhang 2005). Raymond et al. (2006) noted the influence of the MJO during the period they analyzed during the Eastern Pacific Investigation of Climate (EPIC) in 2001, but also describe mechanistically how enhancement of cross-equatorial flow was crucial for increasing surface enthalpy fluxes and invigorating the ITCZ. Enhancement of surface southerlies was not clearly attributable to any particular large-scale disturbance, although the westerly phase of the MJO apparently coincided with their period of investigation. Frank and Roundy (2006) have attributed favorable genesis environments to the MJO, equatorial Rossby waves and mixed Rossby–gravity waves, with perhaps stronger signals in the latter two modes. Thus,

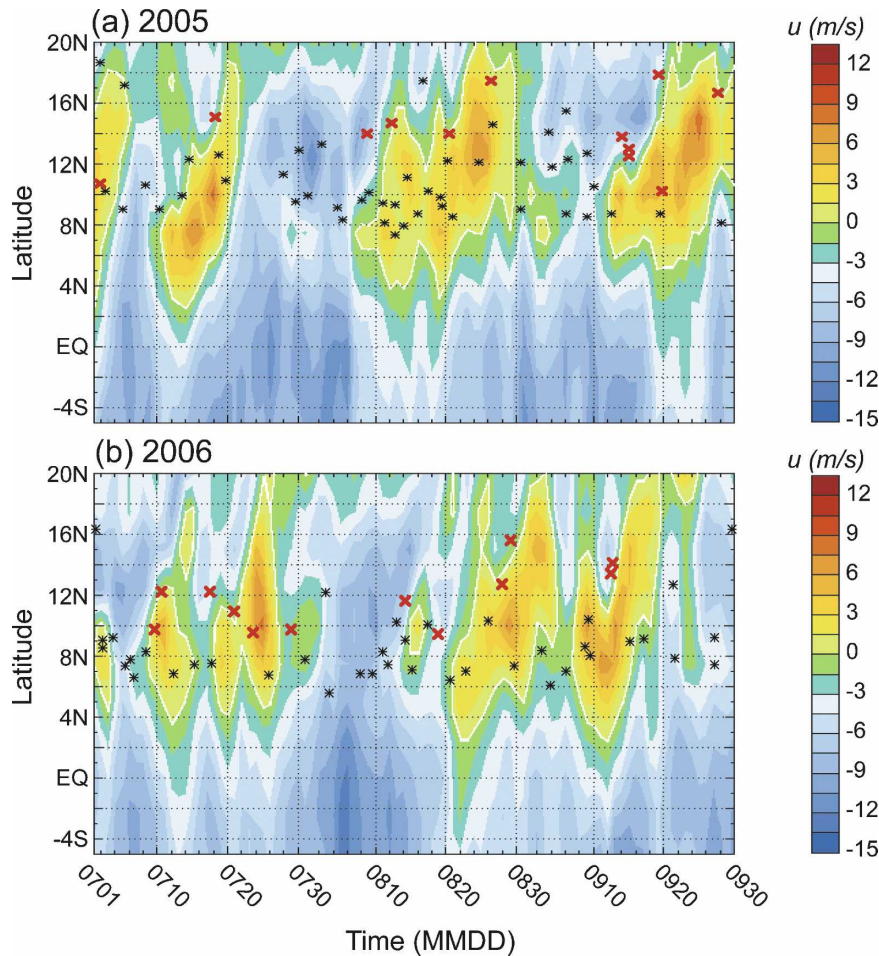


FIG. 8. Time–latitude diagram of zonal wind at 850 hPa, averaged between 140° and 100°W, with positions 24 h after detection of vortices lasting 2 days or more superposed. Red Xs indicate the developing systems and asterisks indicate nondeveloping systems. Time denoted by month (MM) and day (DD). Plot of wind obtained from NOAA/ESRL, Physical Sciences Division.

it appears that more than one wave type may produce the favorable westerly environment in any given time period.

Examining now the meridional and vertical circulation that accompanies lower-tropospheric westerlies, a thermally direct (Hadley) circulation is apparent (Fig. 9a). This cross section represents a composite structure, averaged between 100° and 140°W, for all times at which the 850-hPa zonal wind at 10°N, averaged across the same longitude belt, exceeded 2 m s<sup>-1</sup>. Here, vertical velocity ( $\omega$ ) is computed from integration of the mass continuity equation in pressure coordinates under the assumption of vanishing  $\omega$  at 1000 hPa. This vertical circulation characterizes periods when cyclone development is favored. Comparison of Figs. 8 and 9a indicates that the nondeveloping vortices are more confined to the time-averaged maximum westerlies and

maximum ascent, whereas the developing systems are north of this where both ascent and weak cyclonic shear exist. Note also the vigor of the equatorward flow at 200 hPa, in association with the tropical easterly jet. From this cross section, it is apparent that vertical shear of the meridional wind equatorward of the genesis latitude is a surrogate for the strength of the Hadley circulation.

Interpreting some aspects of Fig. 9a is difficult because individual disturbances are part of the average. It is therefore not clear to what extent Fig. 9a represents an environment for genesis or the result of genesis. This issue is addressed in the context of the meridional circulation later. Here, the collective contribution of individual vortices to the composite meridional profile of absolute vorticity is examined. Having identified the zonal and meridional extents of vortices, the vorticity within a rectangle defined by these dimensions was sub-

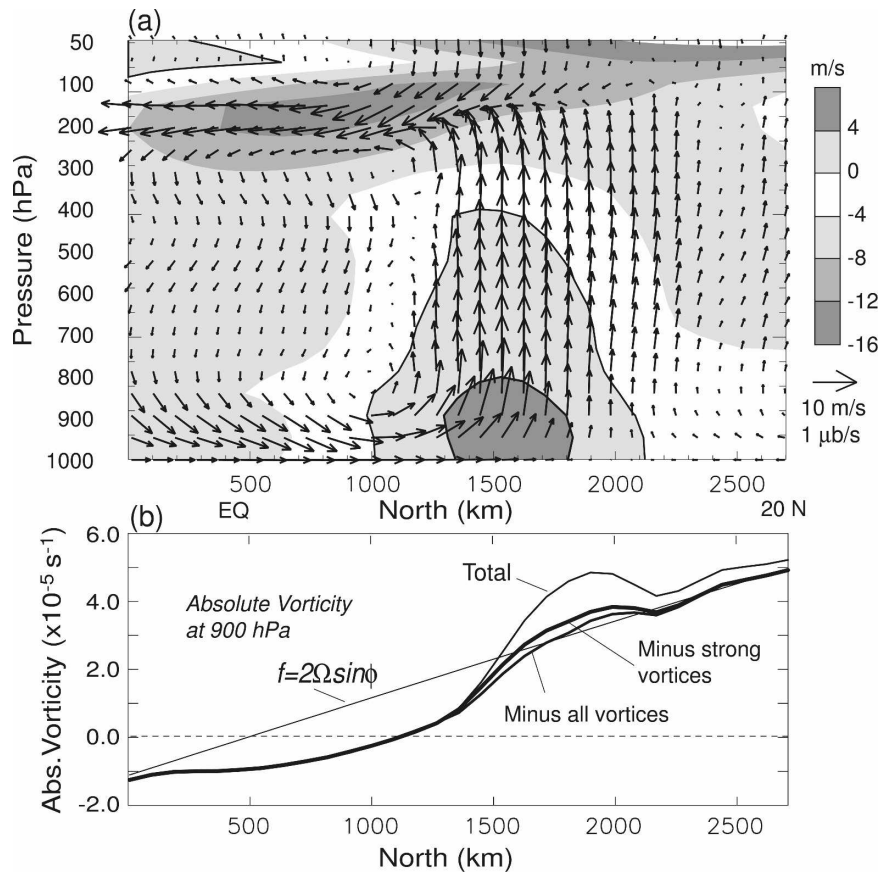


FIG. 9. (a) Mean meridional circulation (vectors) composited for times when the zonal flow averaged between 140° and 100°W at 850 hPa and 10°N exceeds 2 m s<sup>-1</sup>. Shaded is the zonal mean flow, with contours added for positive (westerly) wind. (b) Meridional profiles of relative vorticity corresponding to composite in (a) at 900 hPa. The thin solid line represents mean relative vorticity, the thick solid line represents mean vorticity if vortices exceeding  $5 \times 10^{-5}$  s<sup>-1</sup> are subtracted, and the medium-width line represents mean vorticity if all vortices in the sample are subtracted.

tracted for all vortices in the sample (or portions of vortices that lay between 100° and 140°W). All vortices detected within these longitude bounds were removed at each analysis time. From Fig. 9b it is apparent that this computation removes nearly all the cyclonic vorticity in the domain. In this sense, the mean state is mainly a superposition of discrete vortices.

The above calculation was repeated, but only vortices exceeding  $5 \times 10^{-5}$  s<sup>-1</sup> were removed. The majority of disturbances in this sample were tropical cyclones when they exceeded this threshold. The resulting meridional profile of absolute vorticity is close to the profile obtained with all vortices removed, and also has little cyclonic vorticity remaining. This result implies that the zonal flow during westerly periods is heavily modulated by vortices near and poleward of 10°N. There is also no clear reversal of the absolute vorticity

gradient necessary for barotropic instability of the time-averaged flow with vortices removed. Barotropic instability of the ITCZ has been proposed as a mechanism of eastern Pacific tropical cyclone formation by Guinn and Schubert (1993) and Ferreira and Schubert (1997).

The calculation above made no attempt to formally distinguish vorticity within a vortex from vorticity associated with a synoptic-scale wave and indeed, such a separation is not straightforward. However, from studies such as Maloney and Hartmann (2001), Berry and Thorncroft (2005), and Kiladis et al. (2006), it is apparent that with typical wavelengths of 2000–3000 km and velocity perturbations of several meters per second, the relative vorticity of the wave will typically not exceed  $10^{-5}$  s<sup>-1</sup>. Recall that the spatial extent of the vortex is defined as the distance at which the vorticity drops to 0.2 times its maximum value. For strong vortices, this

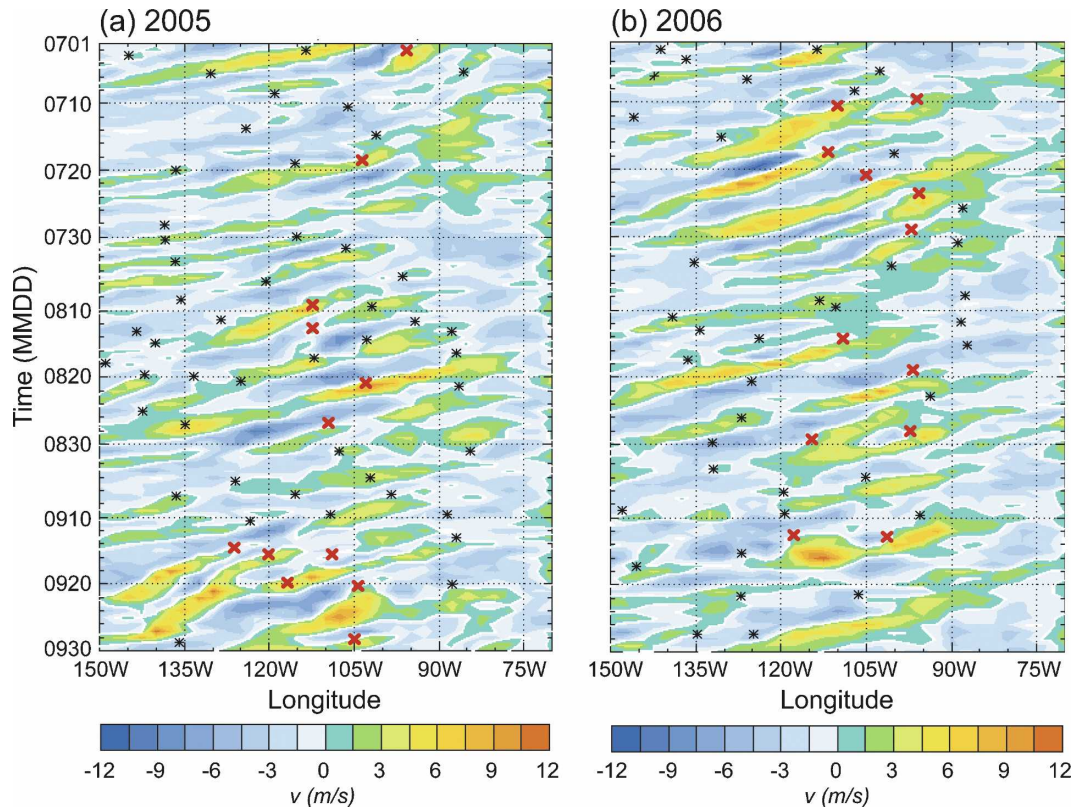


FIG. 10. Time-longitude diagram of 850 hPa meridional wind, averaged between 10° and 15°N, with formation locations of vortices lasting 2 days or more superposed. Red Xs indicate developing systems, and asterisks indicate nondeveloping systems. Time denoted by month (MM) and day (DD). Plot of wind obtained from NOAA ESRL Physical Sciences Division.

minimum value is at least  $10^{-5} \text{ s}^{-1}$ . Thus, the strong vortices rise significantly above vorticity in large-scale waves that might be present. Hence, the results shown in Fig. 9b, for strong vortices, arise primarily due to the removal of coherent vortex structures (with closed contours of vorticity), and to a lesser extent the removal of vorticity projecting onto the structure of synoptic-scale tropical waves.

High-frequency vorticity precursors to genesis typically correspond to couplets of meridional wind moving westward at roughly  $6\text{--}7 \text{ m s}^{-1}$  (Molinari and Vollaro 2000). In Fig. 10, showing time-longitude plots of 850-hPa meridional wind averaged between 10° and 15°N, numerous streaks are evident. Some of the streaks originate over the Atlantic and some first appear around 90°W. Many of the strongest couplets are signatures of hurricanes. It is not clear to what extent these propagating disturbances represent mixed Rossby-gravity waves (MRGs), in the sense of equatorially trapped disturbances (Liebmann and Hendon 1990), or easterly waves propagating on a PV gradient (Molinari et al. 2000). The term “easterly wave” is used in a loose

sense herein to represent westward-propagating disturbances with phase speeds of the order of  $6\text{--}10 \text{ m s}^{-1}$ .

In Fig. 10, as in Fig. 8, the locations of all vortices lasting 2 or more days have been superposed, marked by their position at first detection. While tropical cyclones produce several of the long streaks of meridional velocity anomalies, easterly waves, represented by a temporal couplet in the velocity field, existed prior to the detection of many vortices, both developing and nondeveloping. Furthermore, several vortices were sometimes observed along a single phase line of a wave, for instance, between 12 and 26 August 2005, when five nondeveloping vortices occurred along the same phase line. While easterly waves are perhaps a necessary condition for genesis, their presence does not discriminate developing versus nondeveloping vortices even when they occur during periods of enhanced lower-tropospheric westerlies.

Spatial distributions and parameters following individual vortices will now be examined to better understand what distinguishes developing versus nondeveloping systems. Vertical shear and its spatial distribution

in a vortex-centered domain are examined first, valid 24 h after vortex detection. (Shown in Figs. 12a,b are the fields of composite vector wind shear for the weakest 24 nondeveloping vortices lasting at least 2 days, and the 24 developing vortices, respectively.) The signature of the disturbances themselves is clear in the full shear fields, with strong divergence and anticyclonic rotation apparent in the developing cases. This obscures the environment in which the disturbances are embedded, so a method for removing the disturbance is now described.

Given a field of 900–200-hPa shear vectors, the horizontal “divergence” and “vorticity” of this field are computed. Here divergence is actually the difference in divergence between 200 and 900 hPa (“differential divergence”), positive if there is wind divergence at 200 hPa or convergence at 900 hPa. The vorticity is actually thermal vorticity, or “differential vorticity.” If anticyclonic, as it is in tropical cyclones, it would be balanced by a warm core above a PV maximum. The divergence and vorticity of the vector shear are set to zero outside a radius of 900 km from the vortex center. This radius easily encompasses the scale of disturbances, on average, as illustrated by radial profiles of differential divergence and differential vorticity in Fig. 11. The Poisson equation for the streamfunction in (1) is solved given the differential vorticity perturbation (the field within 900 km of the vortex center), with homogeneous conditions applied on the edge of a domain that is 5400 km on a side. An analogous Poisson equation in (2) is solved for the velocity potential on the same domain given the differential divergence. These boundary value problems can be stated as

$$\nabla^2(\psi_2 - \psi_1) = \begin{cases} \zeta_2 - \zeta_1 & \text{for } r \leq r_0 \\ 0 & \text{for } r > r_0 \end{cases};$$

$$\psi_2 - \psi_1 = 0 \text{ on lateral boundaries,} \quad (1)$$

$$\nabla^2(\chi_2 - \chi_1) = \begin{cases} \delta_2 - \delta_1 & \text{for } r \leq r_0 \\ 0 & \text{for } r > r_0 \end{cases};$$

$$\chi_2 - \chi_1 = 0 \text{ on lateral boundaries,} \quad (2)$$

where  $\psi$  is the streamfunction,  $\chi$  is the velocity potential,  $r_0 = 900$  km, subscript “1” refers to 900 hPa, and subscript “2” refers to 200 hPa. Given solutions for the differential streamfunction ( $\psi_2 - \psi_1$ ) and differential velocity potential ( $\chi_2 - \chi_1$ ), the nondivergent and irrotational wind shear vectors representing the disturbance are

$$\Delta \mathbf{v}_\psi = \mathbf{k} \times \nabla(\psi_2 - \psi_1) \quad \text{and} \quad \Delta \mathbf{v}_\chi = \nabla(\chi_2 - \chi_1). \quad (3)$$

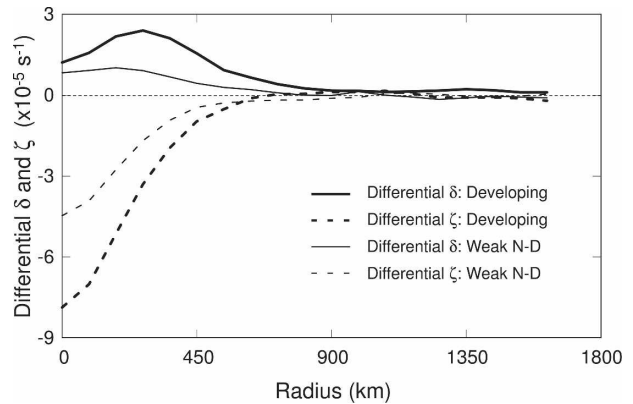


FIG. 11. Radial profiles of differential divergence ( $\delta$ ) and vorticity ( $\zeta$ ), defined as the value at 200 hPa minus the value at 900 hPa, centered on the 900-hPa maximum vorticity 24 h after first detection of a vortex in the GDAS analyses. The thick contours represent developing vortices (24 in sample) and the thin contours represent the weakest 24 nondeveloping vortices that last at least 2 days.

To produce the environmental wind shear (Figs. 12c,d), both  $\Delta \mathbf{v}_\psi$  and  $\Delta \mathbf{v}_\chi$  are subtracted from the total shear vector field:

$$\Delta \mathbf{v}_{\text{env}} = \mathbf{v}_2 - \mathbf{v}_1 - \Delta \mathbf{v}_\psi - \Delta \mathbf{v}_\chi. \quad (4)$$

Based on Figs. 12c,d, it is apparent that the environmental shear in the developing disturbances is larger, particularly to the south of the vortex center. The environmental wind shear pattern clearly indicates a stronger Hadley circulation in developing cases, consistent with greater northerlies in the upper troposphere or southerlies in the lower troposphere, or both, as indicated in Fig. 9a.

Important differences also exist in the 900-hPa vorticity field (Fig. 12). The vortex is stronger in the developing sample by design, but the flanking negative vorticity anomalies are also statistically significant, based on a standard  $t$  test (Wilks 1995) with a threshold of 95% probability of correctly rejecting the null hypothesis. The negative anomaly to the south derives from a stronger northward push of air across the equator in developing cases with near-zero, or negative, absolute vorticity (recall Fig. 3 for Eugene and Fig. 9b). The greater negative vorticity anomaly to the north of the vortex is also statistically significant (confidence as high as 95%). This anomaly is associated with anticyclonic shear vorticity to the northeast of a coastal jet along the west coast of Central America, which may be part of the cyclone circulation itself in some cases (e.g., see Figs. 4b–d).

For each vortex lasting 2 days or more, developing or otherwise, several parameters were computed and av-

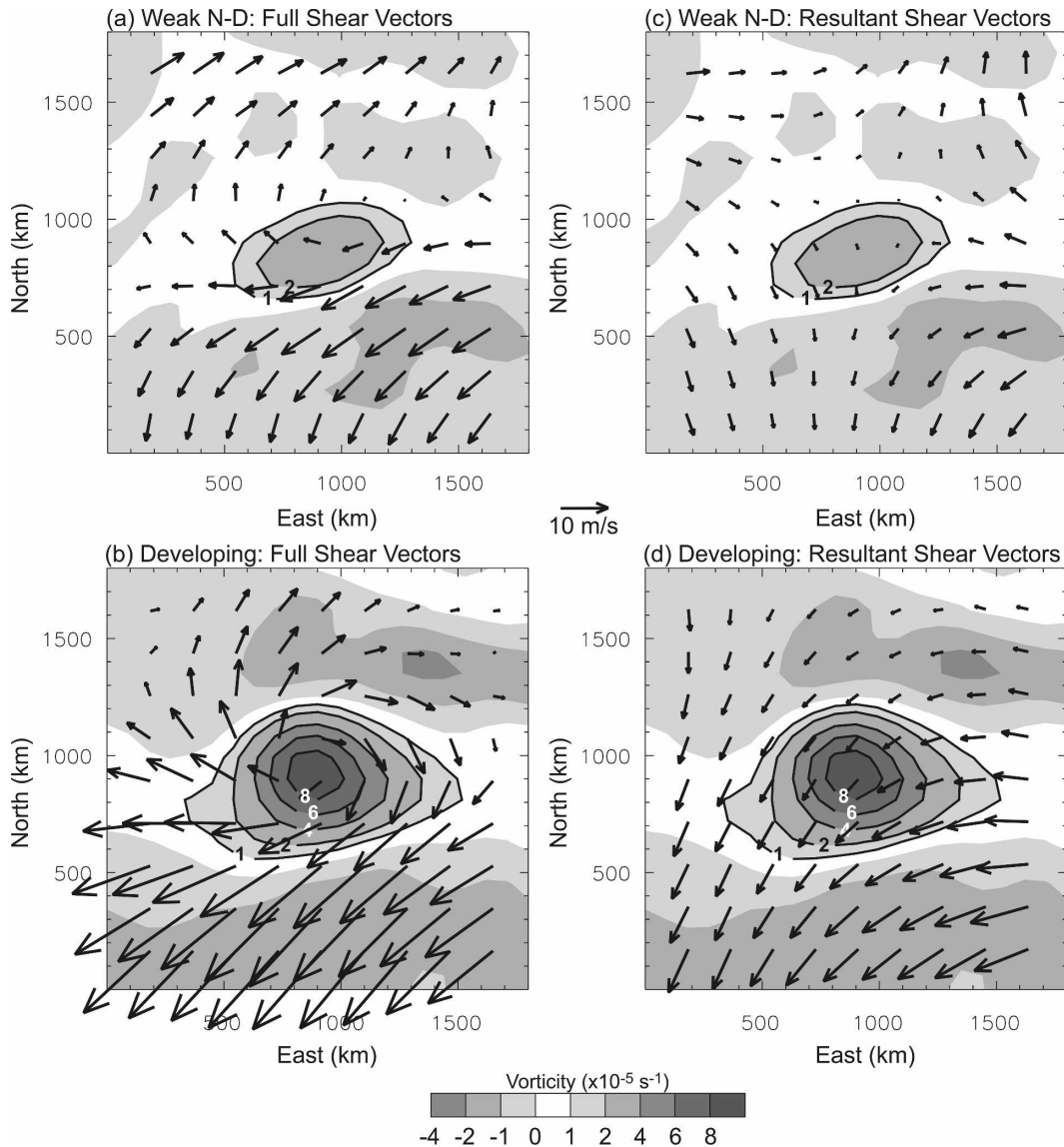


FIG. 12. Harmonic vertical shear between 900 and 200 hPa averaged over (a) the weakest 24 long-lived nondeveloping vortices and (b) the developing vortices. The colored field is relative vorticity at 900 hPa ( $10^{-5} \text{ s}^{-1}$ ). The valid time is 24 h after the initial detection for each case in the composite. Positive relative vorticity is contoured as well as shaded. (c), (d) Same as in (a), (b), but for the resultant shear vectors after the differential vorticity and divergence have been removed.

eraged over the first 48 h following each vortex. These included area averages of vertical shear of the zonal and meridional wind components between 900 and 200 hPa, horizontal stretching deformation at 900 hPa, and 600–900-hPa mean relative humidity. All quantities were area averaged over a box of  $11 \times 11$  grid points, or  $990 \times 990$  km. The vertical shear of the meridional wind component was averaged over a box positioned such that the northern edge passed through the vortex center. This was motivated by the observation that strong northerlies in the upper troposphere occurred

equatorward of developing disturbances (Figs. 1, 9, and 12).

In Fig. 13 histograms of different parameters for developing and nondeveloping samples are shown. The meridional component of vertical wind shear to the south of the vortices (Fig. 13a) turns out to be significantly more negative in developing cases, as determined by the same *t* test as applied to the vorticity in Fig. 12. No developing cases occurred with positive meridional shear (i.e., without the thermally direct Hadley circulation present). On the other hand, the zonal shear

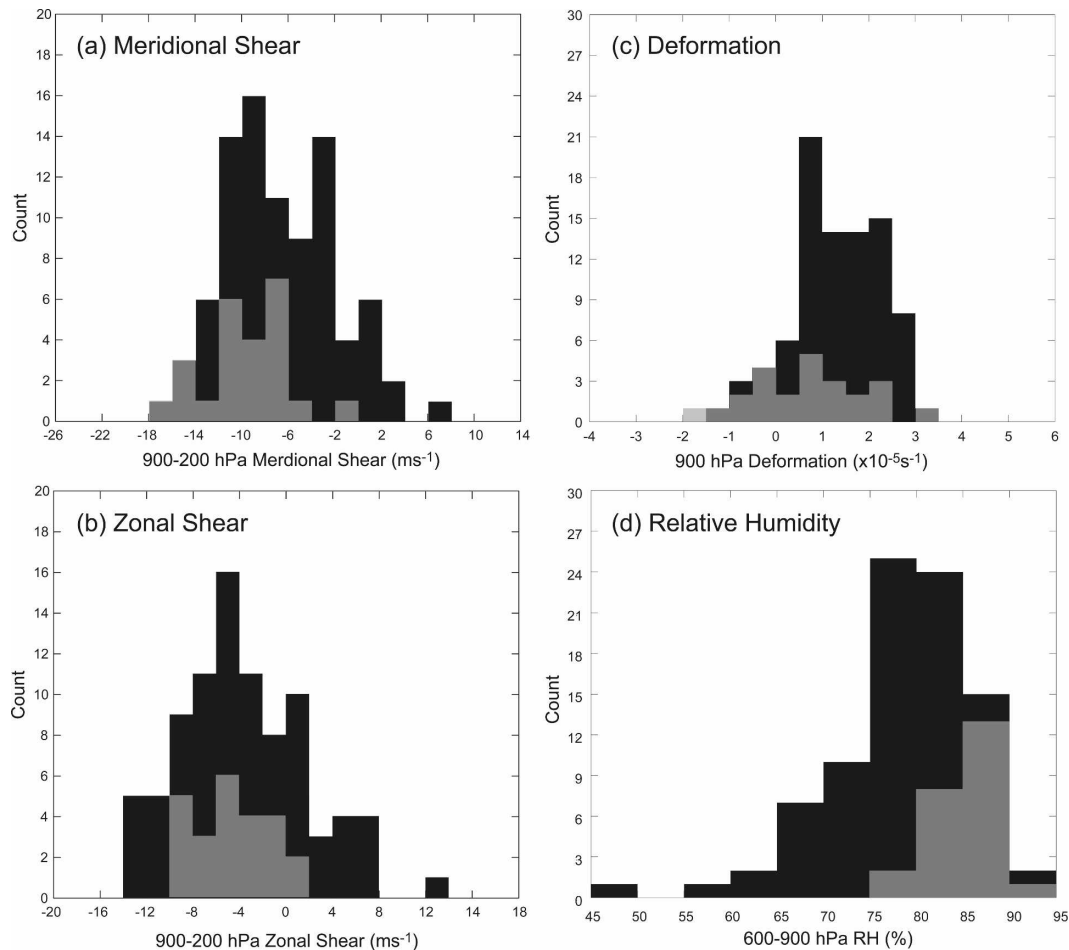


FIG. 13. Histograms of parameters averaged over the first 48 h of the existence of each vortex and averaged over a box  $11 \times 11$  grid points: (a) meridional wind shear between 900 and 200 hPa, (b) zonal shear between 900 and 200 hPa, (c) horizontal stretching deformation at 900 hPa, and (d) relative humidity averaged between 600 and 900 hPa. The box for averaging meridional shear in (a) is displaced so that the northern edge of the box passes through the vortex center. The black bars represent nondeveloping vortices (total of 88) and the gray bars represent developing vortices (total of 24). Light gray shading appears where the number of developing vortices exceeds the number of nondeveloping vortices. Note that the ordinate range in (a), (b) is smaller than in (c), (d).

centered on the vortex (Fig. 13b) showed no significant difference in the two samples. The relative unimportance of the local vertical shear as an indicator of potential development was also found in a larger data sample by DeMaria et al. (2004).

Horizontal stretching deformation  $\partial u/\partial x - \partial v/\partial y$  at 900 hPa (Fig. 13c) differed significantly between the two samples (greater than 95% confidence), with nondeveloping cases featuring positive deformation and developing cases centered near zero deformation. Positive deformation will attempt to zonally elongate vortices. Consistent with this result, it was found that nondeveloping vortices had significantly smaller aspect ratios (the ratio of latitudinal to longitudinal extent) than developing vortices. Because aspect ratio has a non-

Gaussian distribution (not shown) the nonparametric Wilcoxon–Mann–Whitney rank-sum test (Wilks 1995)<sup>3</sup> was used to assess statistical significance. It was also found that during periods of lower-tropospheric westerlies at  $10^\circ\text{N}$  (Fig. 9a), deformation maximized near

<sup>3</sup> In this test, the two datasets are combined and rank ordered. The sum of the ranks of each dataset is computed and the difference in summed rank is compared to an expected difference that one would obtain if both samples were extracted from the same distribution. The statistic tests for the significance of the difference in location (the nonparametric analog of the mean) between the samples. Using this test, we found a greater than a 99% probability of correctly rejecting the null hypothesis that the locations of the two samples were the same.

10°N, but was near zero to the north where development was more common (not shown). The preferential latitude for greater deformation may explain the poleward shift of developing vortices relative to the mean position of the ITCZ and maximum ascent in Fig. 9a.

Considering the relative humidity, averaged between 900 and 600 hPa (Fig. 13d), it is apparent that the humidity in the developing cases is greater and there are no developments with a mean humidity less than 75%. Because the distributions are highly skewed, and evidently non-Gaussian, the nonparametric rank-sum test was used as described above. The confidence for rejecting the null hypothesis exceeded 99.9% for the relative humidity. The higher humidity in developing cases is consistent with stronger upward mass flux on a larger scale as exists within an enhanced meridional overturning circulation. It is also consistent with work by Bister and Emanuel (1997) and Raymond et al. (1998) who showed that genesis is favored in environments of high relative humidity in the lower and midtroposphere because of the suppression of strong downdrafts and their associated boundary layer divergence and the depletion of boundary layer moist entropy.

#### 4. Conclusions

Analyses from the NCEP GDAS for the 2005 and 2006 eastern Pacific hurricane seasons (restricted to July–September) have been utilized to examine synoptic-scale influences on the development of eastern Pacific cyclones. This study distinguishes between developing and nondeveloping vortices. Vortices were detected and tracked based on their magnitude of vorticity at 900 hPa, smoothed over a region 450 km by 450 km, exceeding  $1.5 \times 10^{-5} \text{ s}^{-1}$ .

First, the development of Eugene (2005) was examined. A relatively rapid poleward shift of the ITCZ was observed about 2 days prior to genesis, with a pronounced invigoration of convection. Development occurred poleward of the original ITCZ position and was preceded by a succession of vortices. While the string of vortices qualitatively resembled solutions to the barotropic instability of a PV strip, the development rate of the vortices was several times faster than theoretical results predict.

It was found that both developing and nondeveloping vortices occurred more often when convection along the ITCZ was enhanced in a strong, zonally confined Hadley circulation, with greater near-surface southerlies equatorward of 10°N, and westerlies near 10°N. Nondeveloping vortices also occurred in easterly regimes, but there were no developments with wide-

spread easterly lower-tropospheric flow at 10°N. Within westerly periods, nondeveloping vortices clustered toward the axis of the lower-tropospheric westerlies while developing vortices initiated poleward of these westerlies. The region poleward of the westerlies featured cyclonic vorticity in the time average. However, the time-averaged, cyclonic vorticity itself comprised strong, transient vortices (mainly tropical cyclones). Removing these vortices from the time average resulted in a state with almost no cyclonic vorticity, and no clear reversal of the sign of the meridional gradient of absolute vorticity. Thus, it is not apparent to what extent the enhancement of background vorticity is available to nascent disturbances. Furthermore, it appears that barotropic instability in its classical form is an unlikely mechanism of vortex formation.

There were signatures in vertical shear consistent with an enhanced Hadley circulation that accompanied cyclone formation. Relatively stronger deep-tropospheric northerly shear was found to the south of developing vortices, consistent with this vertical circulation. Consistent with the pattern of vertical shear and the persistent upward motion near 10°N, lower-tropospheric relative humidity was significantly greater in developing cases, on average.

Horizontal stretching deformation in the lower troposphere was larger in nondeveloping cases. Consistent with positive stretching deformation, nondeveloping vortices were more zonally elongated than developing vortices. It is therefore suggested that horizontal deformation is a property of the time-averaged flow that affects the likelihood of development. Furthermore, the observation that deformation maximizes climatologically within the ITCZ may explain the poleward offset of developing vortices relative to this region.

The main conclusion is therefore that there are well-defined synoptic-scale precursors that distinguish developing and nondeveloping tropical vortices. Care has been taken to remove the direct signature of vortices themselves on the flow features considered, thereby focusing on environmental characteristics in a relatively clean way. The present investigation is a first step in a more complete investigation that would consider, for example, interannual variability (including El Niño years), sufficiency of synoptic-scale precursors for development, and cloud signatures distinguishing developing and nondeveloping cases.

The present study has emphasized a vortex perspective of genesis, thereby attempting to separate coherent structures from the background and clarify the role of the synoptic scales. It is possible to see consistency between the wave perspective (e.g., Frank and Roundy

2006) and the vortex perspective. There appears to be a close relationship between the MRG tropical depression (TD) modes and the vortices identified in the present study. This may be similar to the wave–vortex duality of easterly waves over Africa emphasized by Berry and Thorncroft (2005). Frank and Roundy (2006) found that equatorial Rossby waves (ER) coexist with MRG TDs during genesis. Based on their Fig. 8, it is possible that lower-tropospheric southerlies associated with ERs perturb the ITCZ and help establish the invigorated Hadley circulation that defines a favorable genesis environment.

There are several remaining issues regarding reconciling the different and complementary ways in which wave dynamics and vortex dynamics combine to facilitate genesis. The first concerns the dynamics of easterly waves, or MRGs, over the eastern Pacific. Our analysis suggests an abundance of coherent structures, and this begs the question of the role of wave dynamics in these disturbances. The second issue concerns the cause of intraseasonal variations in the eastern Pacific and how much is directly attributable to the MJO. A third, broader issue is whether the convection is a response to waves, modulates waves, or initiates waves. These issues must be resolved to fully interpret the results of Maloney and Hartmann (2001), Molinari et al. (2000), and Frank and Roundy (2006) who demonstrate a clear connection with tropical waves and hurricane genesis.

Little has been mentioned about mesoscale factors on cyclogenesis, such as topographic influences (Farfán and Zehnder 1997) or mesoscale details of the vortices themselves, mainly because the global analyses do not resolve these scales. Despite the apparently large role of the synoptic scale in selecting which vortices will develop, there are some long-lived, strong vortices in the dataset that do not become tropical cyclones (Fig. 6). It is possible that mesoscale details are important for separating these cases from developing cases.

A final, but practically important issue is the predictability of genesis in global models. The fact that there are well-defined synoptic-scale features that favor certain vortices systematically, and that analyses appear to capture vortex precursors to genesis with some fidelity, paints a relatively optimistic picture of predicting the possibility of genesis in the eastern Pacific. This optimism only addresses whether models have intrinsic capability, but does not address the hard requirements of deterministic prediction. An important future effort will be to document the skill of genesis predictions in global models. Furthermore, it will be vital to define the minimal requirements for observations and their assimilation in order to improve the prediction of genesis not only over the eastern Pacific, but in all regions.

*Acknowledgments.* The authors are grateful to Dr. Kristen Corbosiero of UCLA and Professor Lance Bosart of the University at Albany, SUNY, for their helpful comments; Dave Stettner from the Space Sciences Engineering Center at the University of Wisconsin for providing the satellite images; and Mike Black of NOAA's Hurricane Research Division for assistance with the dropsondes data. The manuscript also benefited substantially from the comments of two anonymous reviewers.

#### REFERENCES

- Berry, G. J., and C. Thorncroft, 2005: Case study of an intense African Easterly Wave. *Mon. Wea. Rev.*, **133**, 752–766.
- Bister, M., and K. A. Emanuel, 1997: The genesis of Hurricane Guillermo: TEXMEX analyses and a modeling study. *Mon. Wea. Rev.*, **125**, 2662–2682.
- DeMaria, M., J. A. Knaff, and B. H. Conell, 2001: A tropical cyclone genesis parameter for the tropical Atlantic. *Wea. Forecasting*, **16**, 219–233.
- , C. W. Anderson, J. A. Knaff, and B. H. Connell, 2004: A new product for estimating the probability of tropical cyclone formation. Preprints, *26th Conf. on Hurricanes and Tropical Meteorology*, Miami, FL, Amer. Meteor. Soc., 2C.6. [Available online at <http://ams.confex.com/ams/pdfpapers/75155.pdf>.]
- Farfán, L. M., and J. A. Zehnder, 1997: Orographic influence on the synoptic-scale circulations associated with the genesis of Hurricane Guillermo (1991). *Mon. Wea. Rev.*, **125**, 2683–2698.
- Ferreira, R. N., and W. H. Schubert, 1997: Barotropic aspects of ITCZ breakdown. *J. Atmos. Sci.*, **54**, 261–285.
- Frank, W. M., and P. E. Roundy, 2006: The role of tropical waves in tropical cyclogenesis. *Mon. Wea. Rev.*, **134**, 2397–2417.
- Gray, W. M., 1968: Global view of the origin of tropical disturbances and storms. *Mon. Wea. Rev.*, **96**, 669–700.
- Guinn, T. A., and W. H. Schubert, 1993: Hurricane spiral bands. *J. Atmos. Sci.*, **50**, 3380–3403.
- Halverson, J., and Coauthors, 2007: NASA's Tropical Cloud Systems and Process Experiment. *Bull. Amer. Meteor. Soc.*, **88**, 867–882.
- Kiladis, G. N., C. D. Thorncroft, and N. M. J. Hall, 2006: Three-dimensional structure and dynamics of African easterly waves. Part I: Observations. *J. Atmos. Sci.*, **63**, 2212–2230.
- Liebmann, B., and H. H. Hendon, 1990: Synoptic-scale disturbances near the equator. *J. Atmos. Sci.*, **47**, 1463–1479.
- Maloney, E. D., and D. L. Hartmann, 2000: Modulation of eastern North Pacific hurricanes by the Madden–Julian Oscillation. *J. Climate*, **13**, 1451–1460.
- , and —, 2001: The Madden–Julian Oscillation, barotropic dynamics, and North Pacific tropical cyclone formation. Part I: Observations. *J. Atmos. Sci.*, **58**, 2545–2558.
- McBride, J. L., and R. Zehr, 1981: Observational analysis of tropical cyclone formation. Part II: Comparison of non-developing versus developing systems. *J. Atmos. Sci.*, **38**, 1132–1151.
- Molinari, J., and D. Vollaro, 2000: Planetary- and synoptic-scale influences on eastern Pacific tropical cyclogenesis. *Mon. Wea. Rev.*, **128**, 3296–3307.

- , —, S. Skubis, and M. Dickinson, 2000: Origins and mechanisms of eastern Pacific tropical cyclogenesis: A case study. *Mon. Wea. Rev.*, **128**, 125–139.
- Raymond, D. J., C. Lopez-Carrillo, and L. Lopez-Cavazos, 1998: Case-studies of developing east Pacific easterly waves. *Quart. J. Roy. Meteor. Soc.*, **124**, 2005–2034.
- , C. S. Bretherton, and J. Molinari, 2006: Dynamics of the intertropical convergence zone of the east Pacific. *J. Atmos. Sci.*, **63**, 582–597.
- Rosenthal, S. L., 1967: On the development of synoptic-scale disturbances over the subtropical oceans. *Mon. Wea. Rev.*, **95**, 341–346.
- Rotunno, R., and K. A. Emanuel, 1987: An air–sea interaction theory for tropical cyclones. Part II: Evolutionary study using a nonhydrostatic axisymmetric numerical model. *J. Atmos. Sci.*, **44**, 542–561.
- Wang, C.-C., and G. Magnusdottir, 2006: The ITCZ in the central and eastern Pacific on synoptic time scales. *Mon. Wea. Rev.*, **134**, 1405–1421.
- Wilks, D. S., 1995: *Statistical Methods in the Atmospheric Sciences*. Academic Press, 467 pp.
- Zhang, C., 2005: Madden-Julian Oscillation. *Rev. Geophys.*, **43**, RG2003, doi:10.1029/2004RG000158.